Effects of current generation and electrolyte pH on reverse salt flux across thin film composite membrane in osmotic microbial fuel cells

Mohan Qin [a], Ibrahim M. Abu-Reesh [b], Zhen He [a,*]

[a] Department of Civil and Environmental Engineering, Virginia Polytechnic Institute and State University, Blacksburg, VA 24061, USA
[b] Department of Chemical Engineering, College of Engineering, Qatar University, P.O. Box 2713, Doha, Qatar

A B S T R A C T

Osmotic microbial fuel cells (OsMFCs) take advantages of synergy between forward osmosis (FO) and microbial fuel cells (MFCs) to accomplish wastewater treatment, current generation, and high-quality water extraction. As an FO based technology, OsMFCs also encounter reverse salt flux (RSF) that is the backward transport of salt ions across the FO membrane into the treated wastewater. This RSF can reduce water flux, contaminate the treated wastewater, and increase the operational expense, and thus must be properly addressed before any possible applications. In this study, we aimed to understand the effects of current generation and electrolyte pH on RSF in an OsMFC. It was found that electricity generation could greatly inhibit RSF, which decreased from 16.3 ± 2.8 to 3.9 ± 0.7 gMH when the total Coulomb production increased from 0 to 311 C. The OsMFC exhibited $45.9 \pm 28.4\%$ lower RSF at the catholyte pH of 3 than that at pH 11 when 40 Ω external resistance was connected. The amount of sodium ions transported across the FO membrane was 18.3—40.7% more than that of chloride ions. Ion transport was accomplished via diffusion and electrically-driven migration, and the theoretical analysis showed that the inhibited electrically-driven migration should be responsible for the reduced RSF. These findings are potentially important to control and reduce RSF in OsMFCs or other osmotic-driven processes.

© 2016 Elsevier Ltd. All rights reserved.

1. Introduction

Osmotic microbial fuel cells (OsMFCs) are a new type of microbial fuel cells (MFCs) integrated with forward osmosis (FO) (Zhang et al., 2011). By inheriting the functions of both MFCs and FO, an OsMFC can simultaneously generate electricity and extract water with the aid of a semipermeable FO membrane that rejects solute ions (Cath et al., 2006; Lutchmiah et al., 2014), separates the anode and cathode, and extracts treated water from the anolyte (feed solution) into the catholyte (draw solution) (Lu et al., 2014b; Werner et al., 2013; Yuan and He, 2015). Like regular MFCs, organic compounds in wastewater are oxidized at the anode of OsMFCs by exoelectrogenic microorganisms and the electrons generated from the anode oxidation reaction are transferred to the cathode through an external circuit where oxygen is reduced to water (oxygen reduction reaction) (Zhang et al., 2011). In the past few years, OsMFCs have been studied and developed in the aspects such as substrates and operation optimization. OsMFCs can treat both

synthetic solution and actual wastewater, and it was reported that more than 50% of the treated wastewater could be extracted from the anode (Ge et al., 2013; Ismail and Ibrahim, 2015). Operation optimization focused on selecting the optimal draw solute, determining membrane orientation, and simplifying the cathode. Draw solution (catholyte) plays a key role in the OsMFC operation, and a draw solute that has both a high conductivity and strong buffer capacity will benefit electricity generation and water flux (Ge and He, 2012). The OsMFC having cellulose triacetate (CTA) embedded support exhibited the higher electricity generation due to the less permeability of oxygen than other membranes (Yang et al., 2015, 2016). Air cathodes have been developed to replace liquid cathodes for improving electricity generation in OsMFCs (Werner et al., 2013). In addition, fouling of FO membrane was found to benefit the current generation of an OsMFC despite the reduction of water flux (Zhu et al., 2016). The concept of OsMFCs has also been extended to create osmotic microbial electrolysis cells and osmotic microbial desalination cells (Lee et al., 2015; Zhang and He, 2012).

As a technology based on the principle of FO, the OsMFCs would inherit some intrinsic drawbacks of FO, for example, reverse salt flux (RSF) can hardly be avoided and is one of the most challenging

issues (Phillip et al., 2010). RSF occurs due to a concentration gradient across an FO membrane, resulting in backward transport of draw solutes into the feed side. Such reverse transport reduces the driving force for water transport, increases the operation cost due to loss of draw solutes, and contaminates the feed solution (Cath et al., 2006). RSF can also result in salt accumulation within the fouling layer on the membrane surface, which increases the cake-enhanced osmotic pressure and therefore, exhibits a negative impact on the process efficiency (Boo et al., 2012). In an FO process, an ideal FO membrane should have high water permeability and low solute permeability, to achieve high water flux and low RSF (Cath et al., 2006); however, high water flux usually leads to high RSF (Lutchmiah et al., 2014). For example, the commercial thin-film composite (TFC) FO membrane, which is comprised of an ultra-thin polyamide active layer and a porous polysulfone support layer, is typically more water permeable and has relatively higher RSF compared to conventional asymmetric cellulose acetate (CA) membrane. In an OsMFC, although RSF can decrease the solution resistance and thus benefit the anode activity, overly accumulated salts will negatively influence the microbial activity and impair the quality of the treated effluent, which has been demonstrated in osmotic membrane bioreactors that had decreased organic removal efficiency with accumulated salts due to RSF (Alturki et al., 2012; Lu and He, 2015). Therefore, it is vitally important to reduce RSF for sustainable implementation of FO-based water and wastewater treatment technologies.

A unique feature of OsMFCs, which makes it different from other FO-based technologies, is electricity generation. Compared to conventional MFCs, OsMFCs can generate more electricity under both a batch mode and a continuous mode using either sodium chloride solution or artificial seawater as the catholyte (Ge et al., 2013; Zhang et al., 2011). Such improved performance of electricity generation was attributed to the lower internal resistance of the OsMFCs than that of the MFCs (Werner et al., 2013). An OsMFC mathematical model was developed, and subsequently predicted a reduction of internal resistance with increasing osmotic pressure gradient and water flux, thereby confirming the importance of membrane resistance (Qin et al., 2015). The lower membrane resistance in OsMFCs is related to both a lower pH gradient across the membrane due to the improved proton flux promoted by water flux and higher anolyte conductivity in the presence of reverse salt flux (Zhu et al., 2015). Movement of electrons as a result of bio-electrochemical reactions can affect ion transport across ion exchange membranes (Chen et al., 2012, 2016; Ping et al., 2016). For example, it was reported that the current generation in microbial desalination cells (MDCs) could inhibit back diffusion of ions from the anolyte into the desalinated stream (Ping et al., 2016). In addition, the electric field has been employed to reduce the membrane fouling in membrane bioreactors via the electrostatic repulsion between negative charged foulants and the cathode (Bani-Melhem and Elektorowicz, 2010; Chen et al., 2007; Liu et al., 2013). Thus, we hypothesized that the current generated in OsMFCs could inhibit RSF. A key factor that potentially correlates with both electricity generation and RSF is the electrolyte pH. It has been reported that RSF can vary significantly as a function of solution pH and increase at alkaline pH in the FO process (Arena et al., 2015). The carboxylic acid groups in TFC membrane could gain or lose protons depending on the solution pH, leading to a varied cation transport across the membrane (Holloway et al., 2015); however, it is not clear how this process will be affected by electricity generation.

In this study, we have examined the above hypothesis and aimed to understand the effects of current generation and electrolyte pH on RSF across TFC membranes in an OsMFC. Batch OsMFC experiments were conducted with varied current generation and/

or electrolyte pH. The specific objectives were to: (1) examine whether RSF could be reduced by current generation; (2) investigate how electrolyte pH would affect RSF through interaction with current generation; and (3) reveal the mechanism of RSF and relevant ion transport in the OsMFC.

2. Materials and methods

2.1. OsMFC setup

The schematic of the OsMFC is shown in Fig. S1 and the experimental setup is shown in Fig. S2 (Supplementary materials). The OsMFC consisted of two equal-size compartments ($14 \times 7 \times 3.7$ cm^3/each with a liquid volume of 280 mL) as the anode and the cathode, respectively, separated by a TFC FO membrane (Hydration Technology Innovations, LLC, Albany, OR, USA) with its active layer facing the anode (feed) side. Plastic mesh was placed on both sides of the FO membrane as support materials. Two carbon brushes (Gordon Brush Mfg. Co. Inc., Commerce, CA, USA) were pretreated by being soaked in pure acetone overnight and heat-treated in a muffle furnace (Model 550 Isotemp Series, Fisher Scientific, Pittsburgh, PA, USA) at 450 °C for 30 min; after pretreatment they were inserted into the anode compartment as the anode electrodes. The cathode electrode was a piece of carbon cloth coated with Platinum (Pt) as the catalyst (0.3 mg Pt cm^{-2}). Before use, the TFC membrane was soaked in deionized (DI) water for 30 min according to the manufacturer's instruction (Stillman et al., 2014). The surface area of the FO membrane was about 98 cm^2. A 500-mL bottle was connected to the anode compartment as a reservoir and placed on a digital balance for monitoring water flux. A 300-mL glass bottle containing the catholyte was connected to the cathode as a reservoir. The cathode compartment was aerated with the air to provide oxygen for cathode reaction and create flow turbulence.

2.2. OsMFC operation

The OsMFC was operated at room temperature of ~21 °C. The anode compartment was inoculated with the anaerobic sludge from the Peppers Ferry Regional Wastewater Treatment Plant (Radford, VA, USA). The anode feeding solution contained (per L of DI water): sodium acetate, 0.5 g; NH$_4$Cl, 0.075 g; NaCl, 0.25 g; MgSO$_4$, 0.0075 g; CaCl$_2$, 0.01 g; NaHCO$_3$, 0.05 g; KH$_2$PO$_4$, 0.27 g; K$_2$HPO$_4$, 0.53 g; and trace element, 0.5 mL (Angenent and Sung, 2001). The cathode was fed with 35 g L^{-1} NaCl solution. The OsMFC was operated with 500 mL anolyte and 300 mL catholyte in a batch mode (6 h). After 6-h operation, the data was collected and all the solutions (in both compartments and reservoirs) were replaced. During night, the OsMFC was operated with 1-L anolyte and 500-mL 5 g L^{-1} NaCl solution without data collection for 12 h. The same OsMFC reactor was used for all the tests, to avoid the difference in performance caused by reactor manufacturing. To study the effects of current generation, the external resistance was manipulated to five levels (1 Ω, 10 Ω, 40 Ω, 100 Ω and quasi-infinite (open circuit mode)), and the catholyte pH was fixed at 7 with 1 M HCl solution. In the experiments of controlled catholyte pH, the pH of the draw solution (catholyte) was maintained at 3, 7 or 11 with 1 M HCl or NaOH. In the study of uncontrolled catholyte pH, two experiments were performed: First, the catholyte pH was initially adjusted to 3, 7 and 11 with 1 M HCl or NaOH and 40 Ω external resistance was connected to the OsMFC; second, the external resistance was manipulated to four levels (1 Ω, 10 Ω, 40 Ω and 100 Ω) for different current generation, and the catholyte pH was initially 7 without any further adjustment during the 6-h experiment. The initial pH was adjusted and measured before each experiment. Both the anolyte and catholyte were recirculated at

100 mL min^{-1}. The FO membrane was washed with DI water for removing foulants every 2 days to reduce the effect of membrane fouling on the tests. The integrity tests for the FO membrane with Milli-Q water as the feed solution and 1-M NaCl as the draw solution were performed after each wash. As shown in Fig. S3, neither the water flux nor RSF was significantly changed, suggesting that the FO membrane was relatively stable during the experiment and membrane fouling was reversible. Water permeability coefficients (A) and solute (NaCl) permeability coefficients (B) were determined through the FO tests (Table S1).

2.3. Measurement and analysis

The OsMFC voltage was recorded every 2 min by a digital multimeter (2700, Keithley Instruments Inc., Cleveland, OH, USA). The polarization curve was performed by a potentiostat (Reference 600, Gamry Instruments, Warminster, PA, USA) at a scan rate of 0.2 mV s^{-1}. The pH was measured using a benchtop pH meter (Oakton Instruments, Vernon Hills, IL, USA). The conductivity was measured by a benchtop conductivity meter (Mettler-Toledo, Columbus, OH, USA). The volumetric densities of power and current were calculated based on the liquid volume of the anode compartment, according to a previous study (Zhang et al., 2010). The concentration of chemical oxygen demand (COD) was measured using a DR/890 colorimeter (HACH Co., Ltd., USA) according to the manufacturer's instruction. The catholyte weight in the reservoir was recorded every 1 min on a balance (Scort Pro, Ohous, Columbia, MD, USA) (Wang et al., 2010). The concentrations of Na$^+$ and Cl$^-$ were quantified by using ion chromatography (Dionex LC20 ion chromatograph, Sunnyvale, CA, U.S.A.) equipped with an ED40 electrochemical detector.

The total Coulomb generated in OsMFC was calculated as:

$$Total\ coulomb(\text{C}) = \sum I(A)t(s) \tag{1}$$

where I is electric current and t is the time.

Water flux J_w across the FO membrane (L m^{-2} h^{-1}, LMH) was calculated by the change of catholyte solution weight over time (Wang et al., 2010).

$$J_w = \frac{V_{c,t} - V_{c,0}}{A_m t} \tag{2}$$

where $V_{c,t}$ and $V_{c,0}$ are the volume (L) of the catholyte at the test time t (h) and 0, respectively. The difference of $V_{c,t}$ and $V_{c,0}$ equals to the weight increase of the draw solution in value (kg) during this period; A_m is the membrane area (m^2).

RSF (J_s, g m^{-2} h^{-1}, gMH) from the cathode (draw) to the anode (feed) was calculated based on the salt concentration change in the feed solution (Wang et al., 2010).

$$J_s = \frac{c_{a,t}V_{a,t} - c_{a,0}V_{a,0}}{A_m t} \tag{3}$$

where $C_{a,t}$ and $C_{a,0}$ are the ion concentrations in the feed solution at time t (6 h) and 0, respectively; $V_{a,t}$ and $V_{a,0}$ are the volume (L) of the anolyte at time t (6 h) and 0, respectively.

The pure water permeability coefficient (A, L m^{-2}-h-bar) and salt permeability coefficient (B, m s^{-1}) were calculated as:

$$J_w = A(\pi_D - \pi_F) \tag{4}$$

where π_D and π_F are the osmotic pressure of the draw solution at the membrane interface and osmotic pressure of the feed solution at the feed-membrane interface, respectively (Cath et al., 2013)

and

$$\frac{J_w}{J_s} = \frac{A}{B} nR_g T \tag{5}$$

where n is the number of species that the draw solute dissociates into (e.g., $n = 2$ for NaCl), R_g is the gas constant, and T is the absolute temperature.

The RSF includes diffusion and electrically-driven migration (EDM) according to the Nernst-Planck equation:

$$J_s = J_D + J_M \tag{6}$$

where J_D is the flux due to diffusion and J_M is the flux due to EDM.

Diffusion (J_D) can be calculated by (Phillip et al., 2010):

$$J_{D,i} = -\frac{D_i}{t_M}\left(C_{d,i} - C_{f,i}\right) \tag{7}$$

where D_i is the diffusion coefficient of species i, t_M is the thickness of TFC membrane (m), $C_{d,i}$ is the concentration of species i on the catholyte, and $C_{f,i}$ is the concentration of species i in the anolyte. The diffusion coefficient is calculated as in a previous study (Table S2) (Kim et al., 2007).

The percentage of RSF contributed by Diffusion (J_D) and EDM (J_M) were calculated by Equations (7) and (8), respectively.

$$J_D\% = \frac{J_D}{J_s} \tag{8}$$

$$J_M\% = 1 - \frac{J_D}{J_s} \tag{9}$$

3. Results and discussion

3.1. Current generation decreases RSF

The influence of current generation on RSF was investigated by varying external resistance loading at a fixed catholyte pH of 7. When the external resistance decreased from 100 Ω to 1 Ω, the maximum current density of the OsMFC increased from 16 A m^{-3} to 94 A m^{-3} (Fig. 1A) while the total Coulomb production increased from 90 C to 311 C. During the 6-h operation, the COD concentration in the anode decreased from 411 ± 24 mg L^{-1} to 109 ± 39 mg L^{-1} (mean value ± standard deviation), and the anolyte pH remained relatively stable (7.26 ± 0.17) due to the buffer capacity of phosphate salts. In an open circuit mode, the effluent COD was 207 ± 6 mg L^{-1} while the anolyte pH was 7.10 ± 0.06. The polarization test indicated that there was no obvious power overshoot in the high current zone where low external resistance was applied (Fig. S4); thus, the current generation increased as the external resistance decreased. RSF clearly decreased with increasing current generation (Fig. 1B). In the open circuit mode where there was no current generation and zero total Coulomb, RSF was 16.3 ± 2.8 gMH. Applying an external resistor of 100 Ω to the electrical circuit produced the total Coulomb of 90 C, and decreased RSF to 9.1 ± 2.1 gMH. Further decreasing the external resistance increased current generation and also reduced RSF. The lowest external resistance of 1 Ω resulted in a total Coulomb production of 311 C in a batch; meanwhile, RSF was 3.9 ± 0.7 gMH, a reduction of 76.1 ± 4.3% compared to that of the open circuit condition.

Water flux was not changed significantly with current/Coulomb production (Fig. 1B and Fig. S5), likely due to small change in osmotic pressure difference that resulted in little water flux variation.
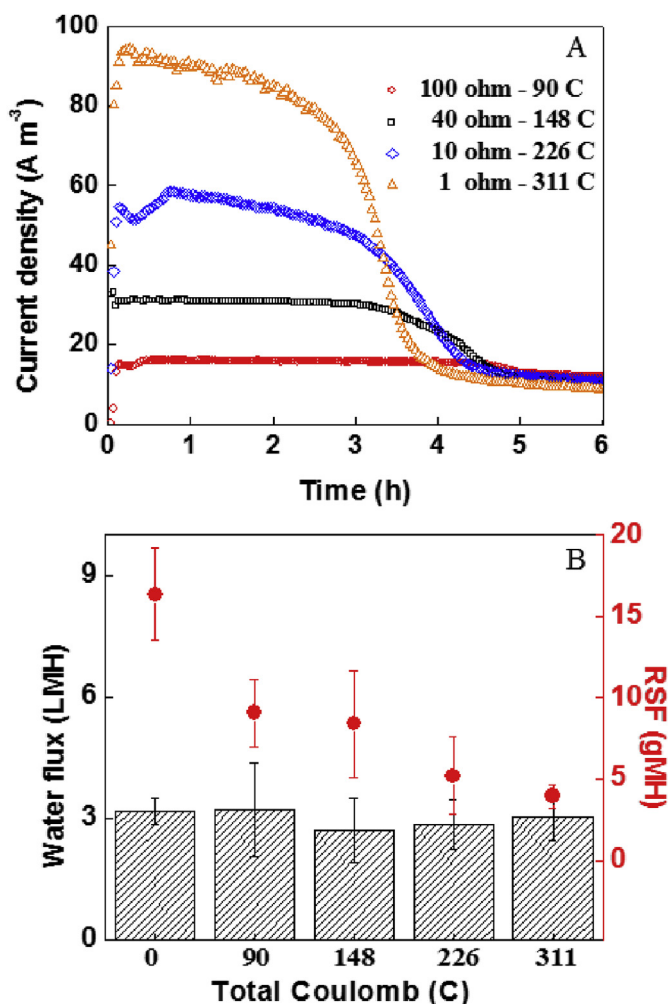
Fig. 1. The OsMFC performance with different external resistance: (A) current generation; and (B) water flux and reverse salt flux (RSF).

Water flux is governed by the osmotic pressure difference ($\Delta \pi$) between the anode (feed) and the cathode (draw), and RSF can reduce $\Delta \pi$ by increasing the anolyte salinity and reducing the catholyte salinity. Dilution of the catholyte due to water extraction would also decrease $\Delta \pi$. After 6-h operation, the osmotic pressure difference in the OsMFC with 3.9 ± 0.7 gMH RSF was 86.3 ± 0.8% of its initial $\Delta \pi$, while it was 78.5± 0.8% of the initial $\Delta \pi$ in the open circuit mode with 16.3 ± 2.8 gMH RSF. The difference in final $\Delta \pi$ between those two conditions resulted from the different RSF, however, the final $\Delta \pi$ difference only contributed to 3.2 ± 0.7 mL water extraction difference, which could be neglected during experimental measurement. Hence, current/Coulomb production did not significantly affect the water flux in the tested OsMFC.

3.2. Effects of controlled catholyte pH

It has been reported that the solution pH can significantly affect RSF in the FO system (Arena et al., 2015). The influence of solution pH on RSF in the OsMFC was investigated with the catholyte pH fixed at 3, 7 and 11, and with external resistance of 10, 40, 100 Ω, and quasi-infinite (open circuit mode), respectively. The anolyte pH was buffered with phosphate buffer solution (initial pH: 7.20 ± 0.04). After the 6-h experiment, the anolyte pH slightly varied to 6.96 ± 0.12, 7.18 ± 0.09 and 7.24 ± 0.24 along with a catholyte pH of 3, 7 and 11, respectively (Fig. S6). The diffusion of H^+

or OH^- from the catholyte to the anolyte might have affected the anolyte pH.

The catholyte pH exhibited strong effects on RSF through interaction with current generation. With the same external resistance, a higher catholyte pH led to a higher RSF (Fig. 2A). For example, when the external resistance was 40 Ω, RSF was 6.6 ± 2.2 gMH, 8.4 ± 3.3 gMH, and 12.2 ± 1.2 gMH at the catholyte pH of 3, 7 and 11, respectively. This difference was related to electricity generation under different pH conditions. The total Coulomb production with 40 Ω was 171 C, 153 C and 142 C at the catholyte pH of 3, 7 and 11, respectively (Fig. 2B). When operated in the open circuit mode (without current generation), the OsMFC showed the highest RSF under every pH (Fig. 2A). A higher catholyte pH would create more potential loss (0.059 V/pH), resulting in lower electricity generation (Zhao et al., 2006). The lower electricity generation would have less inhibition of RSF. In addition, the high pH could affect the membrane surface chemistry, resulting in a higher RSF in an FO process (Arena et al., 2015). The reduction on RSF benefited from current generation was more significant at high catholyte pH. For example, at the catholyte pH of 11, RSF decreased from 18.1 ± 0.7 gMH to 7.0 ± 2.0 gMH when the external resistance decreased from 100 Ω to 10 Ω (the Coulomb production increased from 78 to 241 C, Fig. 2B). This represents 57.0 ± 3.1% reduction in RSF, much higher than 27.8 ± 4.3% (at pH 3) and 42.9 ± 2.5% (at pH 7). Therefore, high current generation could depress the effect of high catholyte pH on RSF.

The effect of the anolyte pH on RSF was not investigated here but may occur. In the anode, the oxidation of the substrates would
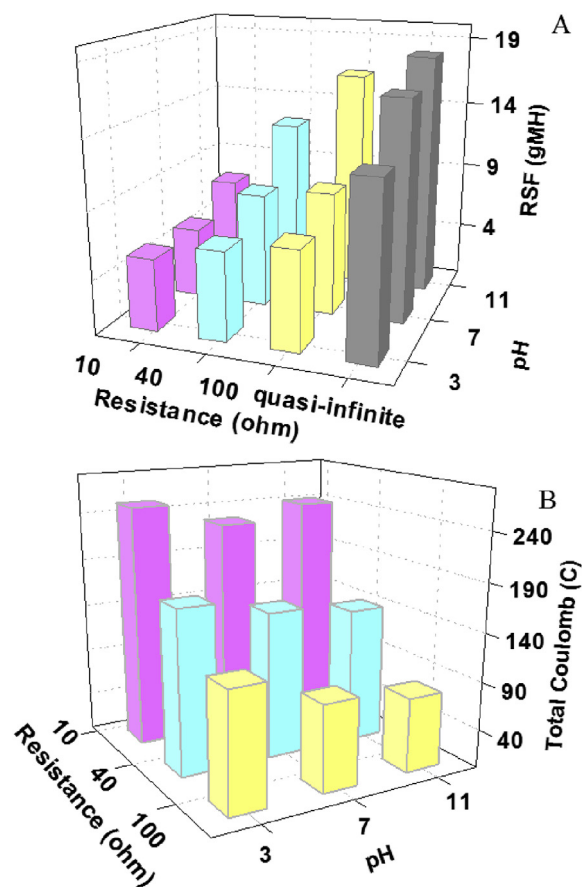

Fig. 2. The effects of the controlled catholyte pH and external resistance: (A) RSF; and (B) total Coulomb production. Quasi-infinite resistance was in the open circuit mode and did not have current generation.

decrease the anode pH due to the generation of proton and lack of buffer capacity. When the anolyte was acidic, the amount of deprotonated carboxylic acid groups would decrease, which may decrease the RSF. However, a lower anolyte pH could inhibit the bioelectrocatalytic activity of anodic microorganisms, increase the internal resistance, and decrease the system stability (Harnisch and Schröder, 2009; Raghavulu et al., 2009). As a result, current generation would decrease and have less inhibition on RSF, thereby resulting in a higher RSF.

3.3. Uncontrolled catholyte pH

In actual operation of an OsMFC, maintaining a fixed catholyte pH would be very difficult because that the draw solutes do not always have a buffer capacity. Thus, we examined RSF and current generation with uncontrolled catholyte pH. Two experiments were performed: the first was to understand the effect of pH variation on RSF at a fixed external resistor and the second test was to investigate the influence of current generation on RSF at initial catholyte pH of 7.

The influence of pH variation on RSF was investigated at external resistance of 40 Ω with three initial catholyte pH: 3, 7 and 11. The solution pH was not adjusted during the 6-h experiment. The RSF was 8.1 ± 1.8 gMH, 8.0 ± 1.9 gMH, and 8.1 ± 1.4 gMH at the initial catholyte pH of 3, 7 and 11, respectively (Fig. S7A), indicating that the RSF was not affected by the initial catholyte pH. These RSF data were consistent with the RSF in the OsMFC at the fixed catholyte pH 7 and same external resistance (8.4 ± 3.3 gMH). In addition, the catholyte pH changed rapidly and became similar at the end of the testing period. Within the first hour of operation, the catholyte pH increased to 8.45 and 8.89 with the initial pH of 3 and 7, respectively, or decreased to 10.22 from the initial pH of 11 (Fig. 3A). At the end of the 6-h operation, the catholyte pH became 8.39, 8.41 and 9.19, with the initial catholyte pH of 3, 7 and 11, respectively. Meanwhile, the current generation was not significantly affected by the initial catholyte pH (Fig. S7B). Therefore, the similar catholyte pH after the 6-h operation resulted in the similar RSF regardless of the initial catholyte pH. The variation of catholyte pH could be related to the dilution effect of the catholyte, oxygen reduction reaction, and proton/hydroxide transport across the membrane. The dilution effect on the catholyte pH due to water flux was very minor, contributing to about 0.2-unit pH change in the catholyte. The final catholyte pH was lower than a theoretical catholyte pH calculated based on the hydroxide ion production (oxygen reduction reaction) from the transferred charge (Fig. 3A) (Werner et al., 2013), indicating that the pH difference could be related to the promoted proton transport. Proton flux could be improved with water flux from the anode to the cathode, which was not considered in the theoretical calculation (Werner et al., 2013). Meanwhile, RSF might stimulate the transport of OH^- from the cathode into the anode for charge neutrality, thereby influencing the catholyte pH.

When there was no current generation in the OsMFC (open circuit), the RSF was 18.7 ± 1.0, 18.2 ± 1.0, and 19.3 ± 1.1 gMH with the initial catholyte pH 3, 7, and 11, respectively (Fig. S8), indicating that the RSF was not affected by the initial catholyte pH in an open circuit mode. The open circuit operations excluded the effect of oxygen reduction reaction on RSF, and there was relatively stable anolyte pH (~7) during the 6-h operation regardless of the initial catholyte pH. In the open circuit mode, the final catholyte pH was 7.05 ± 0.12, 7.10 ± 0.07 and 8.23 ± 0.05 when the initial catholyte pH of 3, 7, and 11, respectively, indicating that the catholyte pH significantly changed during the operation, which could be related to the proton/hydroxide transport across the membrane driven by concentration gradients.
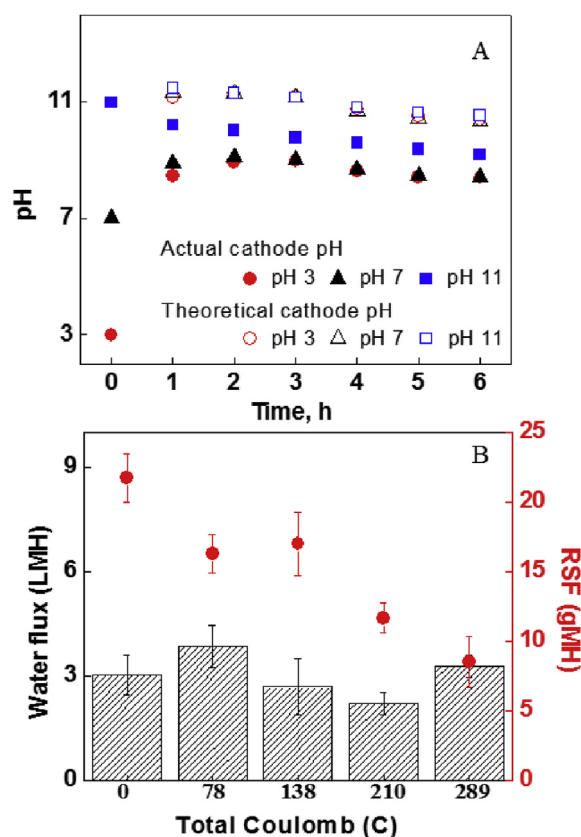

Fig. 3. The OsMFC performance with uncontrolled catholyte pH: (A) measured (actual) and calculated pH value with different initial catholyte pH (external resistance of 40 Ω); and (B) water flux and RSF with different external resistance (initial catholyte pH of 7).

RSF was also examined under different current generation and at an uncontrolled catholyte pH (initially 7). When the external resistance decreased from 100 Ω to 1 Ω, the maximum current density increased from 14 A m^{-3} to 89 A m^{-3} and the total Coulomb production increased from 78 C to 289 C (Fig. 3B). Like the previous test with the controlled catholyte pH, water flux did not change significantly with varied total Coulomb, but RSF significantly decreased from 21.7 ± 1.7 gMH to 8.6 ± 1.8 gMH.

3.4. Ion transport in the OsMFC

RSF is the reverse ion transport of draw solute, which includes both Na^+ and Cl^- in the present OsMFC that used sodium chloride as a draw solute. The mechanism of RSF in the OsMFC was investigated by studying the ion transport (Na^+ and Cl^-) affected by electricity generation and the catholyte pH. The measured concentrations of Na^+ and Cl^- ions were consistent with RSF calculated from conductivity change. As the total Coulomb production increased from 90 C to 226 C, the transport of Na^+ decreased from 20.2 ± 0.1 mmol to 18.7 ± 0.7 mmol, and the transport of Cl^- decreased from 17.0 ± 0.5 mmol to 11.8 ± 1.6 mmol (Fig. 4A). When the (controlled) catholyte pH increased from 3 to 11, the transport of Na^+ increased from 18.2 ± 0.2 mmol to 24.0 ± 1.8 mmol and the transport of Cl^- increased from 13.1 ± 0.8 mmol to 20.0 ± 2.2 mmol (Fig. 4B).

One can observe that Na^+ and Cl^- ions were not transported at an equal amount, and more Na^+ migrated across the FO membrane than Cl^-. TFC membrane could behave similarly to a cation exchange membrane when the carboxylic acid groups in the active
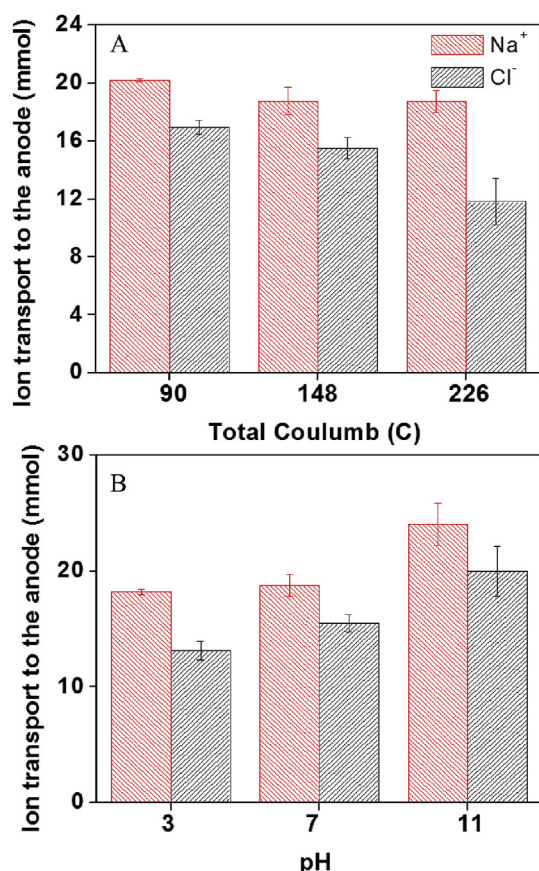
Fig. 4. Transport of sodium (Na$^+$) and chloride (Cl$^-$) ions to the anode: (A) affected by Coulomb production; and (B) affected by the catholyte pH.

layer become deprotonated (-COOH becomes −COO$^-$), which will favor the transport of Na$^+$ and hinder the transport of Cl$^-$ (Arena et al. 2014, 2015; Lu et al., 2014a; Tang et al., 2007). The mechanism of ion transport in the present OsMFC was proposed in Fig. 5. The difference between the transported molar amount of Na$^+$ and

Fig. 5. Proposed mechanism of the ion transport (orange: Na$^+$; green: Cl$^-$) across the TFC membrane. The arrows represent the flux of ions (orange: reverse flux of Na$^+$; green: reverse flux of Cl$^-$ dragged by Na$^+$ transport; yellow: forward flux of Na$^+$ driven by current; purple: reverse Na$^+$ flux inhibited by current; red: increased reverse flux of Na$^+$ by increased catholyte pH). (For interpretation of the references to colour in this figure legend, the reader is referred to the web version of this article.)

Cl$^-$ could be balanced by the forward transport of protons from the anode to the cathode for charge neutrality. When the OsMFC was operated in open circuit, Na$^+$ moved across the TFC membrane from the cathode to the anode due to its high electrostatic attraction to the negatively charged polyamide surface, and dragged the Cl$^-$ across the membrane to maintain the electroneutrality in the anode (Lu et al., 2014a; Phillip et al., 2010). The transport of Na$^+$ was affected by the current generation in the OsMFC, because electrons moving from the anode electrode to the cathode electrode facilitated the forward transport of Na$^+$ (from the anode to the cathode) and inhibited the reverse transport, resulting in a decreased net transport of Na$^+$ from the cathode to the anode. As the total Coulomb production increased from 90 C to 226 C, the percentage of the transported Na$^+$ decreased from 10.1 ± 0.5% to 6.7 ± 0.3%. The decreased Na$^+$ transport could repel the reversed Cl$^-$ transport and thus decrease RSF. As the catholyte pH increased from 3 to 11, more carboxylic acid functional groups became deprotonated, improving negative charge densities on membrane surface that would facilitate cation transport across the membrane, which positively correlated with RSF.

3.5. Mechanism of reduced RSF in the OsMFC

We further studied the salt transport in two mechanisms, diffusion and EDM, according to Nernst-Planck equation. Diffusion was driven by the concentration gradient, while EDM is generated by current or charge difference and can transport certain charged ions (anion/cation) to balance the charge. The analysis shows that the percentage of diffusion and EDM was affected by the current generation and catholyte pH (Fig. 6). In the OsMFC, the electricity
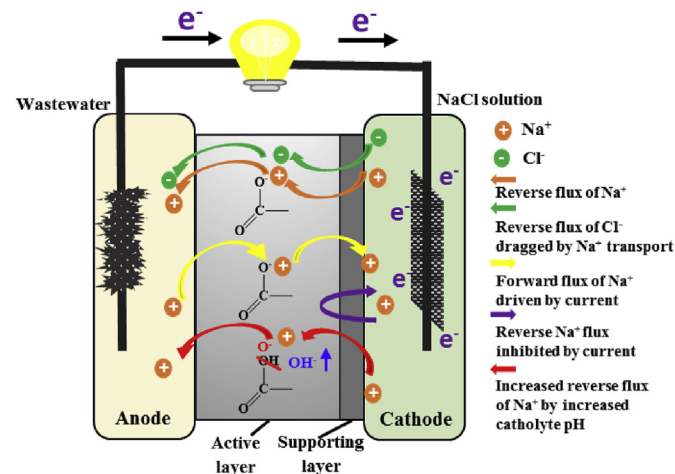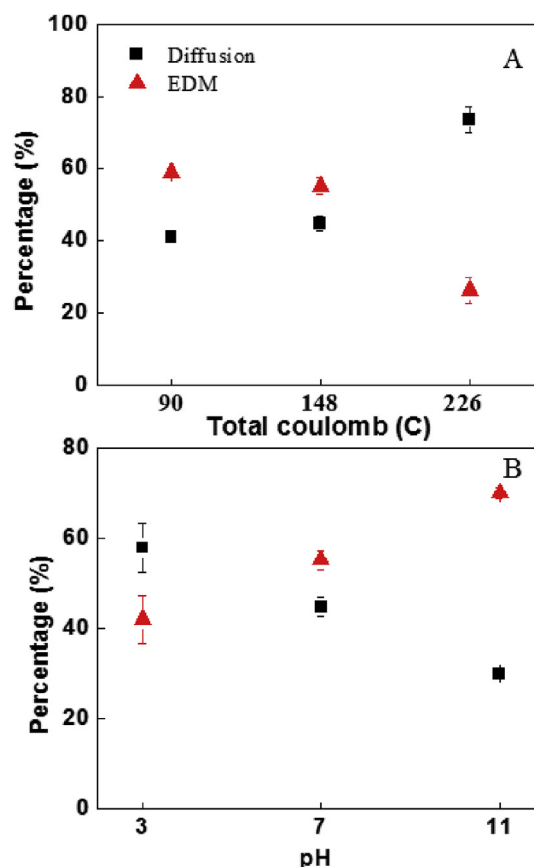

Fig. 6. Contribution of diffusion and EDM (electrically-driven migration) to ion transport: (A) affected by Coulomb production; and (B) affected by the catholyte pH.

generation inhibited the EDM of ions from the cathode to the anode and led to a higher percentage of diffusion. As the total Coulomb production increased from 90 C to 226 C, the percentage of EDM decreased from $59.0 \pm 3.6\%$ to $26.4 \pm 1.2\%$ and the percentage of diffusion increased from $41.0 \pm 3.6\%$ to $73.6 \pm 1.2\%$ (Fig. 6A). RSF decreased along with the current generation was likely due to the reduced EDM. As the current generation (total Coulomb production) increased, more electrons flew from the anode to the cathode. The EDM of Na^+ from the cathode to the anode was in the opposite direction from the electron flow, which would be repulsed and reduced as the increase of electron flow. The contribution of EDM to RSF increased as the catholyte pH increased (Fig. 6B), resulting in a lower RSF in the OsMFC. When the (controlled) catholyte pH increased from 3 to 11, the percentage of EDM increased from $42.1 \pm 5.3\%$ to $70.1 \pm 1.1\%$ and the percentage of diffusion decreased from $57.9 \pm 5.3\%$ to $29.9 \pm 1.1\%$. When the catholyte pH decreased, the deprotonated carboxyl groups in the active layer also decreased, leading to a lower charge difference across the membrane and thus a lower EDM.

In this study, the irreversible fouling of FO membrane was excluded, because of the short-term test and frequent membrane cleaning. However, we should acknowledge that membrane fouling could interact with current generation and pH, with consequent impact on RSF. Previous studies have reported controversial conclusions about the influence of membrane fouling on current generation: Werner et al. found that membrane fouling led to water flux decline but the power generation was unaffected, while Ge et al. and Zhu et al. suggested that the membrane fouling could benefit the current generation (Ge and He, 2012; Werner et al., 2013; Zhu et al., 2016). The membrane fouling could also benefit the forward salt flux, which might result in a reduced RSF (Zhu et al., 2016). Nevertheless, the effects of membrane fouling on current generation and RSF warrant further investigation with actual wastewater and for a long-term operation.

The TFC membrane possesses a cation exchange capability, endowing the function of EDM (electrostatic repulsion) in FO processes when salt ions are used as the draw solutes. However, the electrostatic repulsion in FO membranes is still not well understood (Hancock et al., 2011; Holloway et al., 2015; Lu et al., 2014a; Phillip et al., 2010). When CTA membrane was employed, Hancock et al. (Hancock et al., 2011) and Phillip et al. (Phillip et al., 2010) concluded that the driving force for ion transport was only governed by solute diffusion; however, Lu et al. (Lu et al., 2014a) and Holloway et al. (Holloway et al., 2015) alleged that the electrostatic repulsion is not neglectable in CTA membrane. When TFC membrane was used, the electrostatic repulsion played a more important role in ion transport due to the functional groups (Holloway et al., 2015; Lu et al., 2014a). In the OsMFC with TFC membrane, increased current generation and decreased catholyte pH could suppress EDM (electrostatic repulsion) and thus decrease RSF. This is a new benefit of the OsMFCs that has not been identified before and could have important implications to OsMFC development and applications. For example, the new benefit of RSF reduction will raise the question whether an OsMFC should be operated under high power output (for energy production) or high current generation (for RSF reduction). This will require detailed analysis of potential tradeoff between energy production and the benefit of RSF reduction. It also implies to the general FO field that electricity may be used to control RSF, but the associated energy input must be clearly understood.

4. Conclusions

We have successfully achieved reduced RSF in an OsMFC, and this finding can help with developing an effective strategy for controlling RSF, which is one of the major challenges in FO-based treatment. The main conclusions and results are summarized as:

- Electricity generation could reduce RSF by more than 75%, compared to that of the open circuit (no electricity generation).
- The catholyte pH exhibited strong effects on RSF through interaction with current generation, and a lower catholyte pH would have more RSF inhibition due to higher electricity generation.
- More Na^+ migrated across the FO membrane than Cl^-, because that TFC membrane possessed a certain capacity for cation exchange.
- Two mechanisms, diffusion and electrically-driven migration, were proposed to explain the ion transport across the FO membrane. The electricity generation inhibited the EDM of ions and led to a higher percentage of diffusion.

Appendix A. Supplementary data

Supplementary data related to this article can be found at http://dx.doi.org/10.1016/j.watres.2016.09.028.

References

Alturki, A., McDonald, J., Khan, S.J., Hai, F.I., Price, W.E., Nghiem, L.D., 2012. Performance of a novel osmotic membrane bioreactor (OMBR) system: flux stability and removal of trace organics. Bioresour. Technol. 113, 201–206.

Angenent, L.T., Sung, S., 2001. Development of anaerobic migrating blanket reactor (AMBR), a novel anaerobic treatment system. Water Res. 35 (7), 1739–1747.

Arena, J.T., Chwatko, M., Robillard, H.A., McCutcheon, J.R., 2015. pH sensitivity of ion exchange through a thin film composite membrane in forward osmosis. Environ. Sci. Technol. Lett. 2 (7), 177–182.

Arena, J.T., Manickam, S.S., Reimund, K.K., Freeman, B.D., McCutcheon, J.R., 2014. Solute and water transport in forward osmosis using polydopamine modified thin film composite membranes. Desalination 343, 8–16.

Bani-Melhem, K., Elektorowicz, M., 2010. Development of a novel submerged membrane electro-bioreactor (SMEBR): performance for fouling reduction. Environ. Sci. Technol. 44 (9), 3298–3304.

Boo, C., Lee, S., Elimelech, M., Meng, Z., Hong, S., 2012. Colloidal fouling in forward osmosis: role of reverse salt diffusion. J. Membr. Sci. 390, 277–284.

Cath, T.Y., Childress, A.E., Elimelech, M., 2006. Forward osmosis: principles, applications, and recent developments. J. Membr. Sci. 281 (1), 70–87.

Cath, T.Y., Elimelech, M., McCutcheon, J.R., McGinnis, R.L., Achilli, A., Anastasio, D., Brady, A.R., Childress, A.E., Farr, I.V., Hancock, N.T., 2013. Standard methodology for evaluating membrane performance in osmotically driven membrane processes. Desalination 312, 31–38.

Chen, J., Yang, C., Zhou, J., Wang, X., 2007. Study of the influence of the electric field on membrane flux of a new type of membrane bioreactor. Chem. Eng. J. 128 (2), 177–180.

Chen, S., Liu, G., Zhang, R., Qin, B., Luo, Y., 2012. Development of the microbial electrolysis desalination and chemical-production cell for desalination as well as acid and alkali productions. Environ. Sci. Technol. 46 (4), 2467–2472.

Chen, X., Liang, P., Zhang, X., Huang, X., 2016. Bioelectrochemical systems-driven directional ion transport enables low-energy water desalination, pollutant removal, and resource recovery. Bioresour. Technol. 215, 274–284.

Ge, Z., He, Z., 2012. Effects of draw solutions and membrane conditions on electricity generation and water flux in osmotic microbial fuel cells. Bioresour. Technol. 109, 70–76.

Ge, Z., Ping, Q., Xiao, L., He, Z., 2013. Reducing effluent discharge and recovering bioenergy in an osmotic microbial fuel cell treating domestic wastewater. Desalination 312, 52–59.

Hancock, N.T., Phillip, W.A., Elimelech, M., Cath, T.Y., 2011. Bidirectional permeation of electrolytes in osmotically driven membrane processes. Environ. Sci. Technol. 45 (24), 10642–10651.

Harnisch, F., Schröder, U., 2009. Selectivity versus mobility: separation of anode and cathode in microbial bioelectrochemical systems. ChemSusChem 2 (10), 921–926.

Holloway, R.W., Maltos, R., Vanneste, J., Cath, T.Y., 2015. Mixed draw solutions for improved forward osmosis performance. J. Membr. Sci. 491, 121—131.

Ismail, Z.Z., Ibrahim, M.A., 2015. Desalination of oilfield produced water associated with treatment of domestic wastewater and bioelectricity generation in microbial osmotic fuel cell. J. Membr. Sci. 490, 247—255.

Kim, J.R., Cheng, S., Oh, S.-E., Logan, B.E., 2007. Power generation using different cation, anion, and ultrafiltration membranes in microbial fuel cells. Environ. Sci. Technol. 41 (3), 1004—1009.

Lee, M.-Y., Kim, K.-Y., Yang, E., Kim, I.S., 2015. Evaluation of hydrogen production and internal resistance in forward osmosis membrane integrated microbial electrolysis cells. Bioresour. Technol. 187, 106—112.

Liu, J., Liu, L., Gao, B., Yang, F., 2013. Integration of bio-electrochemical cell in membrane bioreactor for membrane cathode fouling reduction through electricity generation. J. Membr. Sci. 430, 196—202.

Lu, X., Boo, C., Ma, J., Elimelech, M., 2014a. Bidirectional diffusion of ammonium and sodium cations in forward osmosis: role of membrane active layer surface chemistry and charge. Environ. Sci. Technol. 48 (24), 14369—14376.

Lu, Y., He, Z., 2015. Mitigation of salinity buildup and recovery of wasted salts in a hybrid osmotic membrane bioreactor—electrodialysis system. Environ. Sci. Technol. 49 (17), 10529—10535.

Lu, Y., Qin, M., Yuan, H., Abu-Reesh, I.M., He, Z., 2014b. When bioelectrochemical systems meet forward osmosis: accomplishing wastewater treatment and reuse through synergy. Water 7 (1), 38—50.

Lutchmiah, K., Verliefde, A., Roest, K., Rietveld, L.C., Cornelissen, E.R., 2014. Forward osmosis for application in wastewater treatment: a review. Water Res. 58, 179—197.

Phillip, W.A., Yong, J.S., Elimelech, M., 2010. Reverse draw solute permeation in forward osmosis: modeling and experiments. Environ. Sci. Technol. 44 (13), 5170—5176.

Ping, Q., Porat, O., Dosoretz, C.G., He, Z., 2016. Bioelectricity inhibits back diffusion from the anolyte into the desalinated stream in microbial desalination cells. Water Res. 88, 266—273.

Qin, M., Ping, Q., Lu, Y., Abu-Reesh, I.M., He, Z., 2015. Understanding electricity generation in osmotic microbial fuel cells through integrated experimental investigation and mathematical modeling. Bioresour. Technol. 195, 194—201.

Raghavulu, S.V., Mohan, S.V., Goud, R.K., Sarma, P., 2009. Effect of anodic pH microenvironment on microbial fuel cell (MFC) performance in concurrence with aerated and ferricyanide catholytes. Electrochem. Commun. 11 (2), 371—375.

Stillman, D., Krupp, L., La, Y.-H., 2014. Mesh-reinforced thin film composite membranes for forward osmosis applications: the structure—performance relationship. J. Membr. Sci. 468, 308—316.

Tang, C.Y., Kwon, Y.-N., Leckie, J.O., 2007. Characterization of humic acid fouled reverse osmosis and nanofiltration membranes by transmission electron microscopy and streaming potential measurements. Environ. Sci. Technol. 41 (3), 942—949.

Wang, K.Y., Ong, R.C., Chung, T.-S., 2010. Double-skinned forward osmosis membranes for reducing internal concentration polarization within the porous sublayer. Ind. Eng. Chem. Res. 49 (10), 4824—4831.

Werner, C.M., Logan, B.E., Saikaly, P.E., Amy, G.L., 2013. Wastewater treatment, energy recovery and desalination using a forward osmosis membrane in an air-cathode microbial osmotic fuel cell. J. Membr. Sci. 428, 116—122.

Yang, E., Chae, K.J., Kim, I.S., 2015. Comparison of different semipermeable membranes for power generation and water flux in osmotic microbial fuel cells. J. Chem. Technol. Biotechnol. 91 (8), 2305—2312.

Yang, E., Kim, K.-Y., Chae, K.-J., Lee, M.-Y., Kim, I.S., 2016. Evaluation of energy and water recovery in forward osmosis—bioelectrochemical hybrid system with cellulose triacetate and polyamide asymmetric membrane in different orientations. Desalin. Water. Treat. 57 (16), 7406—7413.

Yuan, H., He, Z., 2015. Integrating membrane filtration into bioelectrochemical systems as next generation energy-efficient wastewater treatment technologies for water reclamation: a review. Bioresour. Technol. 195, 202—209.

Zhang, B., He, Z., 2012. Integrated salinity reduction and water recovery in an osmotic microbial desalination cell. RSC Adv. 2 (8), 3265—3269.

Zhang, F., Brastad, K.S., He, Z., 2011. Integrating forward osmosis into microbial fuel cells for wastewater treatment, water extraction and bioelectricity generation. Environ. Sci. Technol. 45 (15), 6690—6696.

Zhang, F., Jacobson, K.S., Torres, P., He, Z., 2010. Effects of anolyte recirculation rates and catholytes on electricity generation in a litre-scale upflow microbial fuel cell. Energy Environ. Sci. 3 (9), 1347—1352.

Zhao, F., Harnisch, F., Schröder, U., Scholz, F., Bogdanoff, P., Herrmann, I., 2006. Challenges and constraints of using oxygen cathodes in microbial fuel cells. Environ. Sci. Technol. 40 (17), 5193—5199.

Zhu, X., Zhang, F., Li, W., Li, J., Li, L., Yu, H., Huang, M., Huang, T., 2016. Insights into enhanced current generation of an osmotic microbial fuel cell under membrane fouling condition. J. Membr. Sci. 504, 40—46.

Zhu, X., Zhang, F., Li, W., Liu, H., Wang, Y., Huang, M., 2015. Forward osmosis membrane favors an improved proton flux and electricity generation in microbial fuel cells. Desalination 372, 26—31.